J. Fluid Mech. (2002), *vol.* 452, *pp.* 405–423.
DOI: 10.1017/S0022112001006772 Printed in the United Kingdom

Gravitaxis in motile micro-organisms: the role of fore–aft body asymmetry

By A. M. ROBERTS AND F. M. DEACON

School of Applied Science, South Bank University, London SE1 0AA, UK

(Received 5 July 1999 and in revised form 28 August 2001)

Scale model experiments on axially symmetric bodies exhibiting fore–aft asymmetry are described. Body shapes are specified by a three parameter equation: two of the parameters (a and b) describe the length and breadth of the body and the third (c) the degree of asymmetry. Objects of this shape orientate as they sediment downwards under gravity until the narrower end lies uppermost, after which they fall vertically downward with no further change in orientation. For the range of parameters investigated the sedimentation velocities, both when vertical and horizontal, are governed principally by a and b, while the rate of orientation is determined by c. The sedimentation characteristics of bodies which cannot be described exactly by the equation can be predicted approximately using best-fit values for a, b and c. These results are applied to consider the role of front–rear asymmetry in ciliated free-swimming micro-organisms. The shape asymmetry is probably sufficient to account for the observed orientation rates in the ciliated protozoan *Paramecium*. It is suggested that these results may be used to deduce the sedimentation behaviour of ciliates from microscope images of individual cells. In small flagellates such as *Chlamydomonas* the orientating effects of the protruding flagella are much larger than the effects of cell body asymmetry. The extreme sensitivity of the orientation rate to slight changes in body shape and flagellar beat patterns may explain why experiments to distinguish between various orientational mechanisms involved in gravitaxis have in the past produced equivocal results.

1. Introduction

The remarkable ability of many types of motile unicellular organisms to swim preferentially upwards (called negative gravitaxis or geotaxis) has been known for well over a century (Verworn 1889; Moore 1903; Jennings 1906; Wager 1911). The effect can readily be demonstrated by stirring a suspension of the ciliated protozoan *Paramecium* in a vertical container; within a few minutes most cells will have swum to the top of the column. Many free-swimming organisms move in what may be described as a biased random walk in which cells repeatedly swim along straight paths for some distance, reorientate spontaneously (tumble) and then move off in some new random direction, and so on. Trajectories between tumbles sometimes have a small helical component because many organisms rotate about their long axis as they swim. Most organisms, being denser than their liquid environment, naturally sediment downwards under gravity, and this downward drift is superimposed on their random movements. In the absence of other effects most organisms would be found at the bottom of their container, with decreasing numbers higher up the water column. In negative gravitaxis, however, tracks actually curve upwards between tumbles which,

if the curvature is sufficiently great, causes net upward swimming by more than compensating for the downward sedimenting effects of gravity. Careful observation of *Paramecium*, for example, shows that tracks curve upward at a maximum rate of orientation (when swimming horizontally) of between 0° and 10° per second (Fukui & Asai 1985; Taneda & Miyata 1995). Gravitaxis occurs both in motile algae and flagellates (which possess one or more long beating flagella that pull the cells through their liquid environment) and in ciliates (which are generally completely covered with much shorter beating cilia that provide their propulsion).

The precise mechanism or mechanisms responsible for curving micro-organism trajectories remains unclear (Hemmersbach, Volkman & Häder 1999). An early suggestion was that orientation was caused by a longitudinal density gradient within the cell, the so-called back-heavy hypothesis (Wager 1911; Dembowski 1931), and this is still considered the most likely orientational mechanism in small flagellated cells such as *Chlamydomonas* (Pedley & Kessler 1992; Jones, Le Baron & Pedley 1994). Another suggestion was that fore–aft body asymmetry, caused either by an asymmetric body shape or by the presence of flagella at one end of the organism, could combine with gravitational sedimentation to orientate cells front-end upward during swimming (Roberts 1970, 1975). These two physical mechanisms can in principle be distinguished by observing what happens when the density of the external medium is increased: shape-dependent orientation should decrease to zero, or even reverse, while back-heavy cells should continue to orientate upwards. Early results were rather inconclusive and contradictory. Fukui & Asai (1980) concluded, on the basis of observations on immobilized specimens of *Paramecium* in sucrose density gradients, that the back-heavy hypothesis can account completely for upward swimming. In contrast, Taneda & Miyata (1995) found that upward orientation decreased to zero as the density of the medium was increased by the addition of heavy water, thereby ruling out the back-heavy hypothesis, at least in this organism. They also found that increasing the viscosity of the medium using methyl cellulose failed to decrease the orientation rate as predicted by the shape asymmetry hypothesis, and concluded that neither hypothesis was able to explain the observations satisfactorily.

Fenchel & Finlay (1984) found that gravitaxis in the freshwater ciliate *Loxodes* switches in sign (from upward to downward active swimming) as the oxygen concentration in the medium is increased. Since no apparent structural changes in the cell were discernible it was concluded that simple physical mechanisms were inadequate, and that *Loxodes* must possess an internal gravity sensor which somehow controls the direction of active swimming. Extensive experiments on several species of micro-organism have now been performed using parabolic aircraft flights, sounding rockets, drop towers and the space shuttle to investigate cell movement in both micro- and hyper-gravity environments (recently reviewed by Hemmersbach *et al.* 1999). The principal new finding is that various chemical agents known to disrupt transduction pathways can affect gravitaxis. Work on the green flagellate *Euglena gracilis,* for example, has shown that inhibitors of stretch-sensitive ion channels inhibit gravitaxis (Lebert & Häder 1996, 1999). Similar results have been found for other organisms. Since it is unclear how the simple physical mechanisms outlined earlier could account for these observations, the biological receptor hypothesis (involving either a discrete internal receptor or gravity-induced stresses in the cell membrane itself) is being increasingly favoured (Hemmersbach *et al.* 1999).

There is some evidence that, having corrected for downward sedimentation of cells under gravity, the ciliates *Paramecium*, *Loxodes* and *Tetrahymena* all swim actively upwards slightly faster than they swim downwards (Machemer *et al.* 1991; Ooya

et al. 1992; Neugebauer *et al.* 1998; Bräucker *et al.* 1998; Kowalewski, Braucker & Machemer 1998; Nagel & Machemer 2000). It has been suggested that this effect, called gravikinesis, is direct evidence for the existence of a gravity receptor inside the cell, possibly in the form of stretch-sensitive channels in the cell membrane which can detect the slight difference in hydrostatic pressure across the cell (Machemer 1994, 1996). However, one difficulty here is that the sedimentation velocity is estimated from measurements on cells which have been immobilized by treatment which is known to change their shape and volume (Kowalewski *et al.* 1998), and this velocity may be rather different to the rate at which normal swimming cells sediment. Another difficulty is that no account has been taken of the fact that sedimentation velocity is likely to depend on the angle of orientation of cells to the vertical.

Two related phenomena in which gravitaxis plays a pivotal role are gyrotaxis and bioconvection. In gyrotaxis a combination of gravity and fluid velocity gradients in the medium causes motile algal cells to converge actively into the centre of a downward moving stream (Kessler 1985; Pedley & Kessler 1987). Bioconvection occurs in dense cultures when characteristic columns of sinking and rising organisms form spontaneously, driven by the cells themselves (Childress, Levandowsky & Spiegel 1975; Pedley, Hill & Kessler 1988; Pedley & Kessler 1992). The study of both these effects has not thrown any light on the actual mechanism of gravitaxis because both back-heavy and shape orientation mechanisms can equally well account for the observations.

Both variable density and shape orientation are well-established hydrodynamic mechanisms which must occur in all free-swimming micro-organisms as they sediment downwards under the influence of gravity. The key question is whether either of these mechanisms is sufficiently large to contribute to the observed effects in gravitaxis. Whenever a cell suddenly expels water from a contractile vacuole, for example, both the density distribution within the cell and the cell shape must change, although the magnitude of the resulting effects may well be small. Much larger cell changes may be caused by osmotic flow when agents such as heavy water and methyl cellulose are added to the external medium. There is currently no method of quantifying the sedimentation characteristics of particular body shapes as seen under the microscope, nor of predicting the consequences of small changes in cell shape.

The principal aim of this work is to investigate how the sedimentation characteristics of cells are affected by cell size and shape, and to re-examine the possible role of shape orientation in gravitaxis in cigar-shaped ciliates such as *Paramecium*. Many species of motile micro-organism have body shapes which resemble slightly distorted prolate spheroids. Prolate spheroids which are denser than their fluid environment sediment downwards under gravity with no change in orientation and with velocities that can be calculated analytically (Happel & Brenner 1973). Distorted prolate spheroids with fore–aft asymmetry, on the other hand, also orientate as they sediment downwards at rates determined by the degree of asymmetry. Since no theoretical analysis has yet been developed for estimating the rate of orientation of such objects as a function of distortion, a sedimentation tank has been used to investigate the behaviour of a series of small aluminium models as they settle downwards through a viscous fluid. The sedimentation tank technique, long used to investigate various aspects of low-Reynolds-number hydrodynamics in general (Happel & Brenner 1973) and in micro-organism movement in particular (Roberts 1970, 1975) has two important advantages in the present context. The behaviour of geometrically similar micro-organisms can be deduced immediately from the model results using the relevant scaling equations, and potential perturbing effects due to the presence of solid walls

can be at least partly accounted for. The experimental results are then used to assess the likely biological significance of shape orientation in swimming micro-organisms.

2. Sedimentation characteristics of asymmetric bodies

The scaling equations which are applicable to the model system can conveniently be derived using the dumb-bell model described by Happel & Brenner (1973). The sedimentation velocity, v, of a single isolated sphere of radius r and uniform density ρ, can be determined by equating the viscous drag (given by Stokes' law when Reynolds number is sufficiently smaller than unity) to the apparent weight (the actual weight less the upthrust in the fluid). Thus

$$\tfrac{4}{3}\pi r^3(\rho - \rho_0)g = 6\pi\eta r v$$

whence

$$v = \frac{2}{9}\frac{(\rho - \rho_0)g}{\eta}r^2, \tag{1}$$

where ρ_0 and η are the density and viscosity, respectively, of the fluid medium and g is the acceleration due to gravity. Two spheres of radius r_1 and r_2 and of the same density ρ are now connected by a light, rigid inextensible rod. When the dumb-bell is inclined at an angle to the vertical it follows from (1) that the larger sphere on the dumb-bell sediments downwards (if $\rho > \rho_0$) more rapidly than the smaller, and stable equilibrium is eventually reached with the dumb-bell axis vertical and the larger sphere beneath the smaller.

If the hydrodynamic interaction between the spheres is ignored, the steady downward velocity, $v_\parallel$, of the model when its long axis is vertical (i.e. sedimenting 'end-on') is given by

$$v_\parallel = \frac{2}{9}\frac{(\rho - \rho_0)g}{\eta}\left(\frac{r_1^3 + r_2^3}{r_1 + r_2}\right).$$

If the total length of the model is L, and if $e = r_1/L$ and $f = r_2/L$, the equation can be written in the form

$$v_\parallel = \frac{2}{9}\frac{(\rho - \rho_0)g}{\eta}L^2\left(\frac{e^3 + f^3}{e + f}\right)$$

or, in general,

$$v_\parallel = \frac{(\rho - \rho_0)g}{\eta}L^2 F_\parallel, \tag{2}$$

where $F_\parallel$ is a dimensionless shape factor which is independent of size.

It is also of some interest to obtain an estimate of the sedimentation velocity of the dumb-bell at the instant it is horizontal, because this is a parameter that can readily be measured in biological cells. Since the dumb-bell is orientating in this position as it drops, the instantaneous velocity varies from one end to the other. An indication of the sedimentation velocity at the instant the dumb-bell's longitudinal axis is horizontal (i.e. sedimenting 'broad-side on'), $v_\perp$, is given by the average velocity of the two spheres:

$$v_\perp = \frac{2}{9}\frac{(\rho - \rho_0)g}{\eta}L^2(e^2 + f^2)$$

or

$$v_\perp = \frac{(\rho - \rho_0)g}{\eta}L^2 F_\perp \tag{3}$$

where $F_\perp$ is another scale-independent shape factor.

The orientational characteristics of the asymmetric dumb-bell can be deduced in the same way. Similar arguments show that the angle between the long axis of the dumb-bell and the vertical, α, varies with time according to the equation

$$\frac{\mathrm{d}\alpha}{\mathrm{d}t} = -\beta \sin(\alpha), \tag{4}$$

where β, the maximum rate of orientation when the long axis is horizontal ($\alpha = \pi/2$), is given by

$$\beta = \frac{(\rho - \rho_0)g}{\eta} L F_\alpha, \tag{5}$$

where the shape factor F_α is also to be determined experimentally.

These results are only indicative of the general behaviour of asymmetric objects because the hydrodynamic interactions between the two ends of the dumb-bell have been ignored. However, Happel & Brenner (1973) have given complete analytical solutions for the hydrodynamic drag on a prolate spheroid of semi-major and semi-minor axes a and b moving both parallel and perpendicular to the long axis. The two sedimentation velocities are given by (2) and (3) above, the shape factors being given by

$$F_\parallel = \frac{1}{48\phi}\left[\frac{-2\phi}{\phi^2 - 1} + \frac{2\phi^2 - 1}{(\phi^2 - 1)^{3/2}} \ln\left(\frac{\phi + \sqrt{\phi^2 - 1}}{\phi - \sqrt{\phi^2 - 1}}\right)\right] \tag{6}$$

and

$$F_\perp = \frac{1}{48\phi}\left[\frac{\phi}{\phi^2 - 1} + \frac{2\phi^2 - 3}{(\phi^2 - 1)^{3/2}} \ln\left(\phi + \sqrt{\phi^2 - 1}\right)\right], \tag{7}$$

where $\phi = a/b$. The effect of including the complete hydrodynamic interaction is just to change the shape factor in the sedimentation equations.

Since the volume of a prolate spheroid is given by

$$V = \tfrac{4}{3}\pi a b^2$$

then (1) for a prolate spheroid can be written in the form

$$v_\parallel = \frac{6M(\rho - \rho_0)g}{\pi \eta \rho L} \phi^2 F_\parallel, \tag{8}$$

where M is the mass of the spheroid. This form of the equation is particularly useful for scale model work because M can be measured accurately, and the shape of the model now determines only the hydrodynamic drag.

The relevant scaling equations for inferring the sedimentation behaviour of an organism from observations on a geometrically similar model become

$$\frac{v}{v_m} = \frac{\Delta\rho}{\Delta\rho_m} \frac{\eta_m}{\eta} \left(\frac{L}{L_m}\right)^2, \tag{9}$$

where v now applies to both $v_\parallel$ and $v_\perp$, and

$$\frac{\beta}{\beta_m} = \frac{\Delta\rho}{\Delta\rho_m} \frac{\eta_m}{\eta} \frac{L}{L_m}, \tag{10}$$

where the subscript m refers to the model parameters.

3. Model construction

A total of 44 small aluminium models (density $2710\,\mathrm{kg\,m^{-3}}$) were turned on a computer-controlled lathe and finished by hand. Their widths were all approximately 6.0 mm, their lengths ranging between 14 and 23 mm and their masses between 0.6 and 1.2 g. Profiles were generated on the lathe using the three-parameter equation

$$r(\theta) = \frac{ab}{\sqrt{a^2 \sin^2(\theta) + b^2 \cos^2(\theta)}} + c\cos(\theta), \tag{11}$$

where the first term on the right describes an ellipse with semi-major and semi-minor axes of lengths a and b, and the second term confers a degree of fore–aft asymmetry specified by the length c. The models themselves are solids of revolution about the $\theta = 0$ axis. The length of each model, L, is given by $L = 2a$, the maximum width being determined by both b and c. This profile equation was chosen rather than a more conventional Fourier expansion in θ because the profile reduces, with no asymmetry, to a prolate spheroid for which the analytical expressions (6) and (7) are available. The volume can readily be calculated numerically from the profile equation. Parameter values were chosen to cover the range of cell shapes likely to be encountered in practice ($0.25 < b/a < 0.4$ and $0.02 < c/a < 0.08$). Typical profiles generated by (11) are illustrated in figure 1.

Digitized images were taken of each model using a Ricoh RDC-300 camera, and downloaded into a data-processing package (Mathcad 7 with image processing add-in) to determine the boundary pixel coordinates. This was done by binarizing the image, dilating by one layer to give another image, and subtracting the two images to identify the boundary pixels. A least-squares procedure was then used to fit the boundary to (11). The origin of an (r, θ) coordinate system was first positioned arbitrarily somewhere inside the body profile. Values of $r(\theta)$ were calculated for each boundary point and compared with corresponding values predicted by (11) for given a, b and c. The sum of the squared deviations in $r(\theta)$ was then minimized, using a nonlinear optimization algorithm, by adjusting the position of the coordinate origin and the values of a, b and c to find the best-fit curve.

Two methods were used to estimate the goodness-of-fit to the model profile. The first was by comparing the best-fit curve with the photographed outline. On the computer screen the fit for the computer-generated models seemed extremely good, although there was a tendency in some models for one end to deviate slightly from the required shape where the model had been parted by hand on the lathe. The root-mean-square deviation in $r(\theta)$ between the profile and the fitted curve, expressed as a percentage of the half-length a (and called here the degree of mismatch), was typically about 0.5%, corresponding approximately to one pixel width in the image. The second method was to calculate the mass of each model from the measured a, b and c values using the profile equation (11) and the known density of the model, the standard deviation of the percentage differences between calculated and measured mass being about 3%. Interestingly, quite large discrepancies were found between the best-fit parameters and the nominal dimensions fed into the computer-controlled lathe, and consequently the best-fit parameters were used to characterize the models rather than the nominal dimensions.

4. Experimental procedure

Observations were made on the aluminium models as they sedimented down the central axis of a square-sided glass tank containing glycerol (density $1260\,\mathrm{kg\,m^{-3}}$).

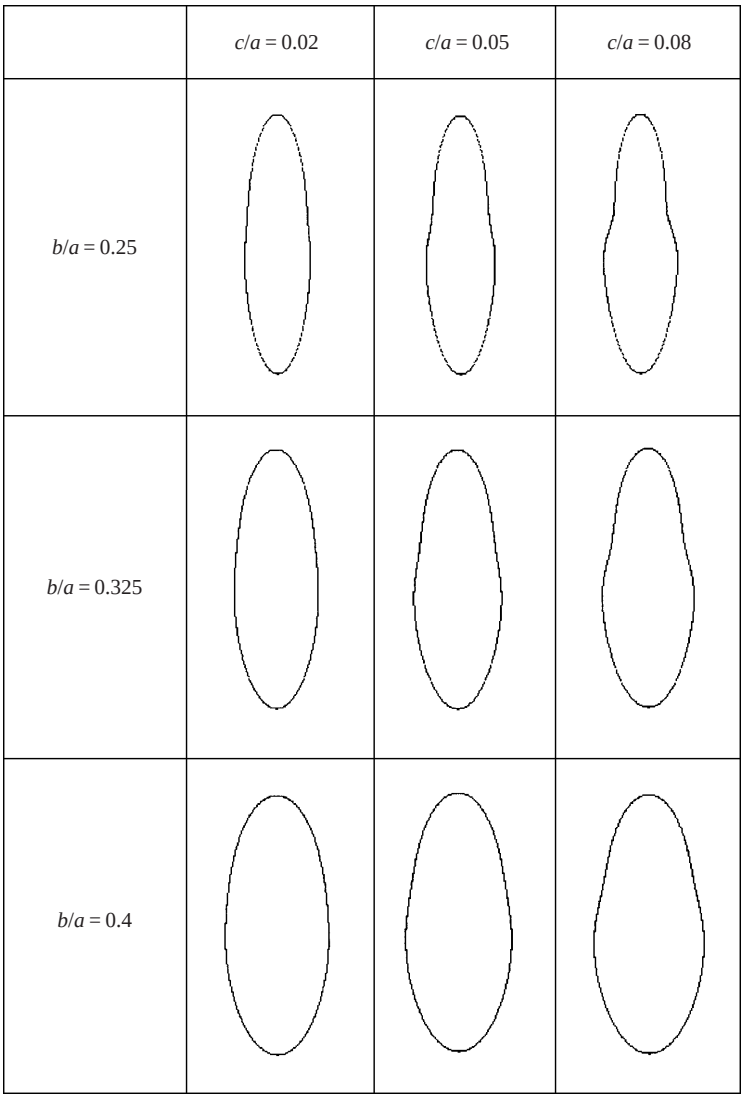

FIGURE 1. Typical model body profiles generated by equation (11) covering the range $0.25 < b/a < 0.4$ and $0.02 < c/a < 0.08$. Profiles of specimens of the ciliate *Paramecium caudatum*, seen under the microscope, most closely resemble the four profiles nearest the top left-hand corner of the diagram, the precise size and shape depending on the age and condition of the culture and the state of the medium.

Most measurements on swimming cells are made on micro-organisms swimming between microscope slides typically 2 mm apart, and an organism such as *Paramecium*, for example, is therefore never further than five body lengths away from a solid wall. The models used in these experiments varied in length between 14 and 23 mm, and the tank size was chosen so that models moving down along its central axis were between 3.5 and 6 body lengths away from the nearest walls (horizontal cross-section 160 mm square, glycerol depth 240 mm).

Experiments were conducted in a cold room maintained at 5 °C as a convenient means of maximizing the viscosity of the glycerol. A number of ball bearings, with

diameters of between 1 and 3 mm, were timed (using a stop clock) as they fell through the middle third of the liquid column as indicated by parallel markers inscribed on the sides of the tank. No significant differences could be detected between the viscosities calculated using (1) for the various sizes of ball bearings, implying that wall effects, which should increase the apparent viscosity for the larger sizes, were too small to be detected. Glycerol viscosity was routinely determined using 1 mm diameter ball bearings. During the series of experiments the viscosity decreased from about 4 to 3 Pa s due to absorption of atmospheric moisture by the glycerol, and the viscosity was monitored before, during and after each set of measurements.

The scale models were held using cooled forceps just beneath the surface of the glycerol on the tank axis and then released. Drop times of vertically orientated models were measured manually using a stop clock. The experimental error associated with the velocity measurements is estimated to be about 2%. For the orientational measurements, models were held with cooled forceps at appropriate angles (α) to the vertical, with their wider ends uppermost and in the vertical plane at right angles to the video camera (Panasonic S-VHS model AG-455B) used to record their subsequent descent. Each model exhibits similar behaviour during descent. The long axis rotates through the horizontal until the model is falling with its narrower end uppermost. The models also drift sideways, first one way until the long axis is horizontal, then back again as the descent continues. The maximum lateral displacement is always less than half a body length. The release angle (α) was chosen for each model so that it reached the horizontal position when halfway down the tank. The video records were analysed using a video capture card (Intel Indeo 2.1) and image processing software (Mathcad) to yield values of the velocity of the model mid-point ($v_\perp$) and angular rotation (β) at the instant the long axis was horizontal. This was done by marking, in each video frame, the positions of each end of the model, then calculating the instantaneous orientation of the long axis and the position of the mid-point. These were both plotted against time, the values of $v_\perp$ and β being estimated from the graphs. This was not a very accurate process: the models had to be imaged over some distance as they fell through the tank, and the images of the models in each video frame were small (typically 10 pixels).

5. Results for the computer-generated models

5.1. *Sedimentation velocities*

Vertically aligned models were released at the top of the tank with their smaller ends uppermost and timed manually as they sank without change in orientation through the middle 100 mm of the fluid column, several determinations being made in each case. The measured velocities ($v_\parallel$) were first compared with predictions made using (8) for prolate spheroids with known masses and measured values of b/a. Figure 2 shows the measured sedimentation velocity plotted against the calculated velocity for each model, and figure 3 shows the percentage difference between the two velocities plotted against the asymmetry parameter c/a. The standard deviation of the percentage differences is 2.4%, consistent with the experimental uncertainties of measurement. The asymmetry has no discernible effect on the sedimentation velocity. The hydrodynamic drag on each model is the same as that on a prolate spheroid of the same a and b values, at least for the range of b/a and c/a values used and within the limits of accuracy of these experiments.

This result is of little use to the microscopist, who may want to infer the sedimen-

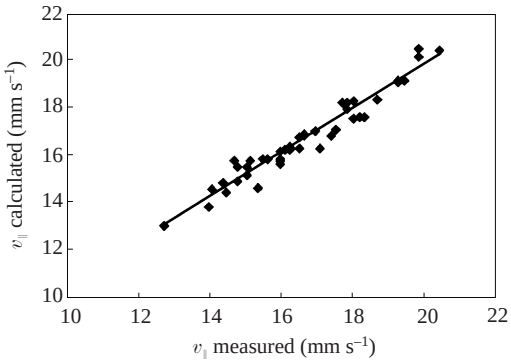

FIGURE 2. Experimental sedimentation velocities of distorted prolate spheroid models falling with vertical orientation ($v_\parallel$) plotted against velocities calculated using (8) with the best-fit values of a and b and the model masses. $R^2 = 0.95$.

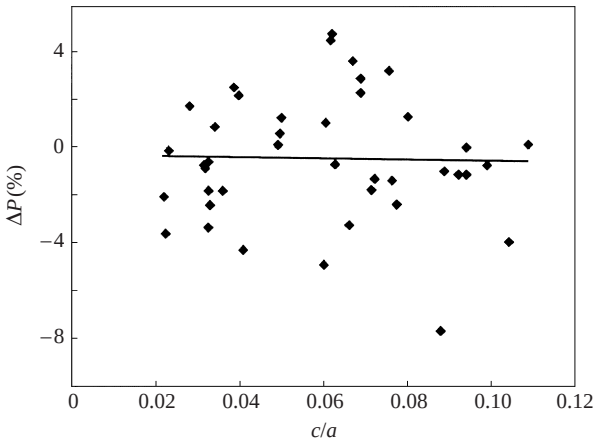

FIGURE 3. Percentage difference (ΔP) between calculated and measured sedimentation velocities ($v_\parallel$) plotted against c/a for the distorted spheroid models. There is no significant dependence on c/a. $R^2 = 0.004$.

tation velocity for a given cell size and shape but does not know the mass of the cell. If the parameters a and b have been determined, (2) together with (6) can be used to estimate $v_\parallel$ provided the cell density is known. Velocities calculated in this way for the aluminium models give a similar result to that shown in figure 3, although the standard deviation of the differences is now slightly higher, as would be expected, at about 3%. Figure 4 shows the percentage differences between measured and calculated velocities plotted against Reynolds number based on the length of each model. There is no evidence of any significant discrepancies at higher Reynolds numbers, which would have implied violation of the usual low-Reynolds-number approximation assumed in this work. No wall effects were discernible in these experiments for vertically orientated translation down the central axis of the tank.

The sedimentation velocity of models at the instant they are horizontal is also of some experimental interest. Measured values of $v_\perp$ for each body are shown plotted against the Happel & Brenner results for prolate spheroids with the same a and b values (figure 5). Also shown (figure 6) is a graph of the percentage differences between measured and calculated $v_\perp$ values using (8), plotted against c/a. Agreement

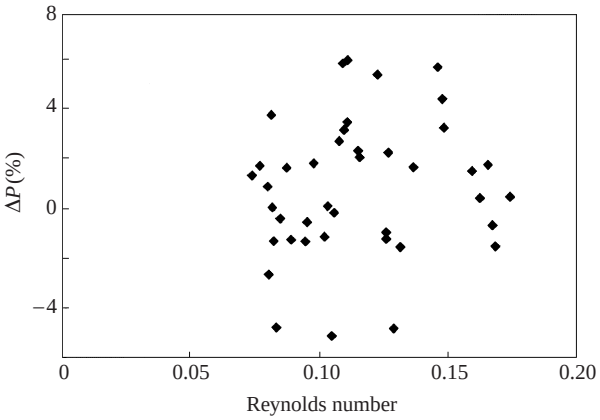

FIGURE 4. Percentage difference (ΔP) between calculated and measured sedimentation velocities ($v_\parallel$) plotted against Reynolds number for the distorted spheroid models; $R^2 = 0.023$. There is no evidence of significant differences between theory and measurement at the higher Reynolds number, which would have implied violation of the usual low Reynolds number approximation used here. For comparison, a specimen of *Paramecium* sedimenting passively under gravity and then swimming at $1\,\mathrm{mm\,s^{-1}}$ in normal aqueous medium has Reynolds numbers based on length of about 0.02 and 0.22 respectively.

between the two sets of results is again good, although the standard deviation of the differences is now greater at about 4% of the mean value. The greater scatter in the experimental results arises because $v_\perp$ could not be determined to the same degree of accuracy as $v_\parallel$, partly because of the inherent errors involved in digitizing the video record and partly because both instantaneous sedimentation velocity and angular velocity vary continuously with orientation to the vertical. The results show that $v_\perp$ depends significantly on c/a ($P = 0.011$) together with a significant wall effect ($P = 0.008$) which shows as a reduction in measured velocity compared to the calculated velocity at $c/a = 0$. The best-fit formula for $v_\perp$ therefore becomes

$$v_\perp = W\frac{(\rho - \rho_0)g}{\eta}L^2F_\perp(1 + (0.6 \pm 0.2)c/a), \tag{12}$$

where W is the wall correction factor estimated from figure 5 to be about 0.960 ± 0.015, corresponding to an average reduction (over all models) in sedimentation velocity of about 4% due to the presence of the tank walls.

It may be supposed that the weak dependence of $v_\perp$ on c/a (a 6% increase in $v_\perp$ as c/a increases from 0 to 0.1) is an artefact caused by choosing the mid-point to measure the velocity rather than the centre of mass. Since the centre of mass of each model is further from the narrower end than the mid-point (as can be seen by inspection of figure 1), its velocity, $v_\perp^C$, will always be greater than $v_\perp$ by an amount which depends on the horizontal rotation rate, β. Expressing equation (12) in terms of $v_\perp^C$ would therefore produce a larger c/a dependence, not a smaller one. Another factor that could cause the observed dependence is that the masses of models of given b/a increase slightly as c/a increases, and this, as equation (8) indicates, will also increase the velocity for given b/a. The increase is estimated to be about 1.5% over the range $0 < c/a < 0.1$, insufficient to account for the observations. It therefore appears that the c/a dependence is a small but real effect.

Prolate spheroids fall more slowly when dropping broadside on. A cell with $b/a \sim 0.3$ (such as *Paramecium*, for example) sediments downwards 20% slower when

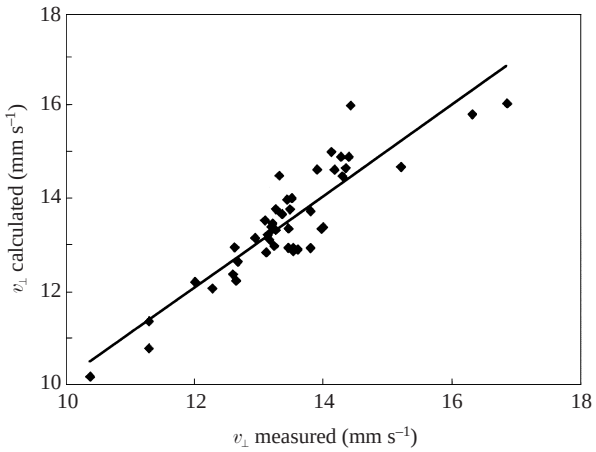

FIGURE 5. Experimental sedimentation velocities for horizontal orientation ($v_\perp$) plotted against velocities calculated using the measured model masses and the best-fit values of a and b. $y = 0.99x + 0.18$, $R^2 = 0.81$.

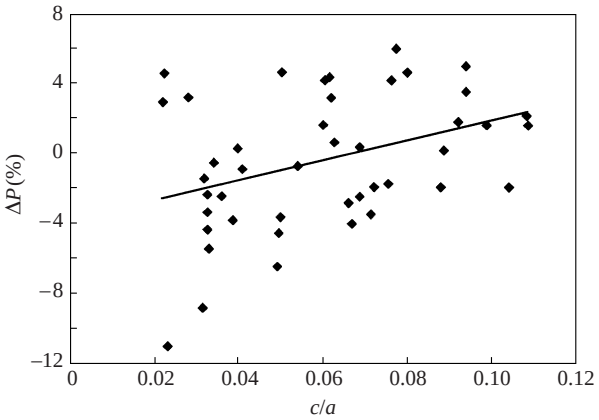

FIGURE 6. Percentage difference (ΔP) between measured and calculated sedimentation velocities ($v_\perp$) plotted against c/a for the experimental models. There is a small but significant dependence on c/a, and also a detectable wall effect. The slope of the best-fit line is $(58 \pm 22\%)$ and the intercept is $(-3.9 \pm 1.4)\%$; $R^2 = 0.144$.

horizontal than when vertical. The downward component of velocity $v(\alpha)$ at angle α is given in general by

$$v(\alpha) = v_\parallel - (v_\parallel - v_\perp)\sin^2\alpha$$

(Happel & Brenner 1973), and this dependence on α should perhaps be taken into account when analysing sedimentation velocities in cells.

These observations apply only to swimming organisms. Immobilized cells invariably have distorted body shapes (lateral body asymmetry or bend in the long axis of the cell) and tend to settle with a range of orientations to the vertical. In a swimming (rotating) cell these should average out, however, and the present model results should be applicable. It is probably unsafe to infer the sedimentation characteristics of swimming cells from measurements on immobilized cells.

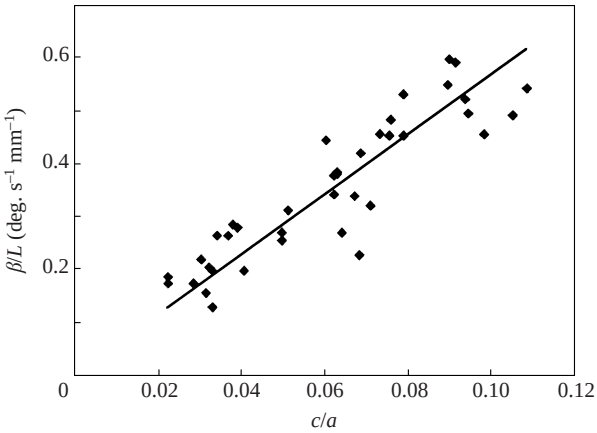

FIGURE 7. Values of β/L plotted against c/a for the distorted prolate spheroid models. The best-fit line is drawn through the origin. The slope of the best-fit straight line is $(5.6 \pm 0.6)^\circ\,s^{-1}\,mm^{-1}$. Measured orientation rates have been scaled using (9) to a viscosity of 4.0 Pa s. $R^2 = 0.80$.

5.2. *Angular reorientation during sedimentation*

The expectation from (5) is that the maximum rate of orientation, β, is proportional to L for bodies of the same shape, and may depend on both (b/a) and (c/a). The experimental results were therefore fitted to the regression model

$$\frac{\beta}{L} = A + B\frac{b}{a} + C\frac{c}{a},$$

yielding values of the constants (best value $\pm$ SEM) as $A = (-0.007 \pm 0.060)$, $B = (0.18 \pm 0.18)$ and $C = (4.8 \pm 0.4)$. The orientation rate β/L depends significantly only upon c/a, and the relation between them is displayed in figure 7. A best-fit straight line has been drawn through the origin, and it is assumed that within the accuracy of the experiment, β/L is proportional to c/a. The value of the constant F_α in (5) is calculated from the slope of the graph to be $F_\alpha = (0.028 \pm 0.002)(c/a)$, and, since $L = 2a$ for these models, (5) now becomes

$$\beta = (0.056 \pm 0.004)\frac{\rho - \rho_0}{\eta} gc, \tag{13}$$

where β is in rad s^{-1}.

It is known that flagella protruding from cells are also a cause of hydrodynamic orientation (Roberts 1975) and it is of interest to compare the magnitudes of the two effects. A thin wire was attached to the rear of one of the aluminium models and the orientation rate measured as its length was reduced in stages (figure 8). The maximum rate of flagellar orientation occurs when the tail length is roughly equal to the length of the cell, and completely swamps the orientational effects of body shape. In this model a tail of only 15% of the body length is sufficient to cancel completely the effects of shape orientation due to body asymmetry. In small flagellated cells such as *Chlamydomonas*, which has flagella of order of body size protruding forward, flagellar orientation will always predominate over the effects of body asymmetry.

Finally, the question arises of whether the presence of the tank walls has any significant influence on the rates of orientation of the models in these experiments. Cylindrical rods dropped into the tank sedimented downwards without any tendency to orientate, even though drifting off the central axis towards one of the tank walls,

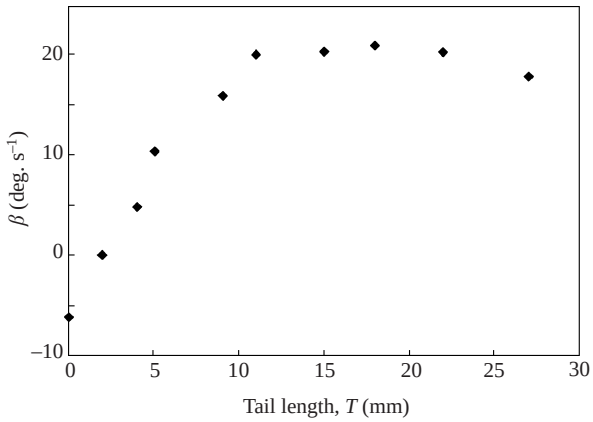

FIGURE 8. Measured maximum orientation rates (β) for an aluminium model ($L = 14.25$ mm, $b/a = 0.39$, $c/a = 0.11$) with tails of diameter 0.6 mm and of various lengths T attached to its rear. Glycerol viscosity was 3.1 Pa s.

and it it unlikely that the orientations observed are caused by the walls themselves. Orientation rates may well be somewhat different in an unbounded fluid, but since swimming micro-organisms are always observed near solid boundaries the orientation rates measured in the tank are probably of greater biological relevance. Orientation rates will certainly be modified when cells sediment close to the walls, but this question has not been investigated here.

6. Sedimentation characteristics of axisymmetric bodies with fore–aft asymmetry and arbitrary profile

The results presented above show that the sedimentation rate in the asymmetric prolate spheroid models is primarily determined by a and b whilst the orientation rate is determined by c. It is of interest to enquire whether the sedimentation characteristics of bodies of not too dissimilar shape can be estimated by finding the best-fit values of a, b and c and then using the results obtained above for distorted prolate spheroids. It would be particularly useful, for example, to be able to predict the sedimentation characteristics of ciliates from their microscope images. A series of measurements was therefore undertaken on twelve aluminium models of arbitrary shape and of various lengths, with masses in the range 50–1500 mg. Their body profiles are shown in figure 9.

Photographed profiles were fitted to (11) to obtain best-fit values of a, b and c for each model, as before. The goodness of fit is now obviously much worse, the degree of mismatch ranging between 3% and 12%. An example of a fitted profile is shown in figure 9. Their sedimentation characteristics were determined as before. Predicted values of $v_\parallel$, $v_\perp$ and β were derived using (2), (12) and (3) together with the best-fit values of a, b and c. The results are shown in figures 10–12. On average, these models sedimented downwards (both $v_\parallel$ and $v_\perp$) slightly faster (by about 4% on average) than predicted by (2) and (12), although the standard deviation of the differences between models was about 10%.

The graph of β against c suggests proportionality, as before (figure 12). The straight line in the graph shows the orientation rate predicted by (3) with slope

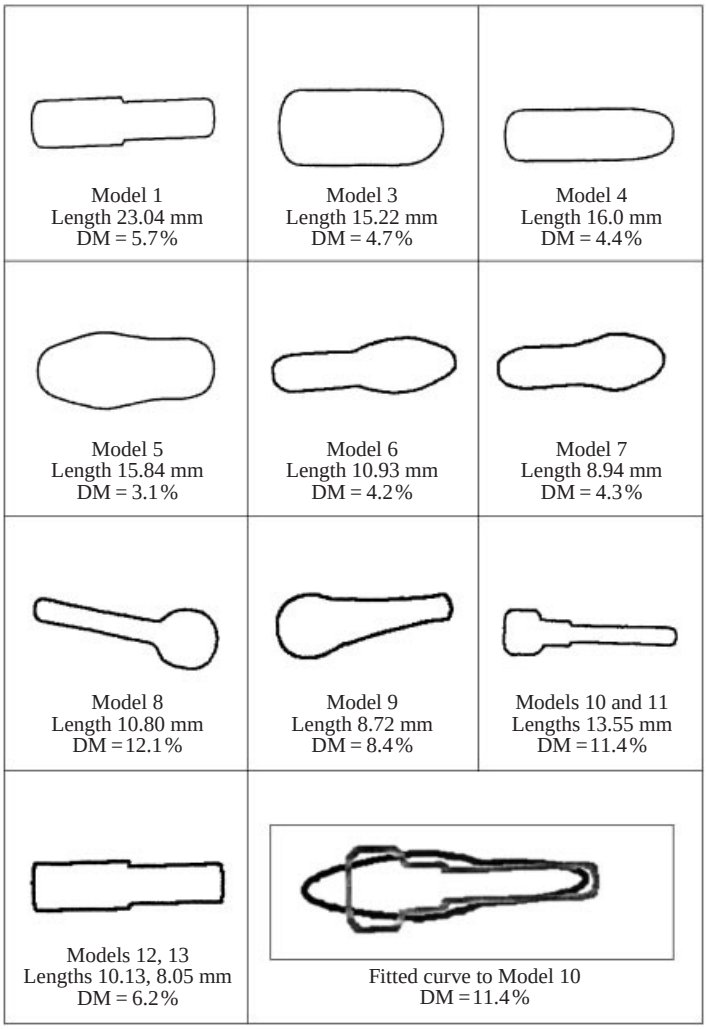

FIGURE 9. Profiles of models with arbitrary shapes. The degree of mismatch (DM) between body profile and the fitting equation (11) is shown for each model.

$(11.4 \pm 0.5)^\circ\,s^{-1}\,mm^{-1}$. The best-fit straight line to the data (not shown in figure 12) has slope $(13.5 \pm 1.7)^\circ\,s^{-1}\,mm^{-1}$, the difference not being significant ($P = 0.25$).

It appears that the results applicable to prolate spheroids may be applied with a fair degree of accuracy ($\pm 10\%$) to estimate both the sedimentation velocity and orientation rates of objects which are not too dissimilar to the standard shapes described by (11). It could therefore be the basis of a general method for predicting the sedimentation characteristics of swimming ciliates.

7. Discussion

These scale model results suggest that the sedimentation properties of motile ciliated cells may be quantified, at least approximately, by the application of these scaling equations to microscopic images of cells. A number of difficulties are apparent, however. Some organisms possess an elliptical cross-section; *Loxodes striatus*, for

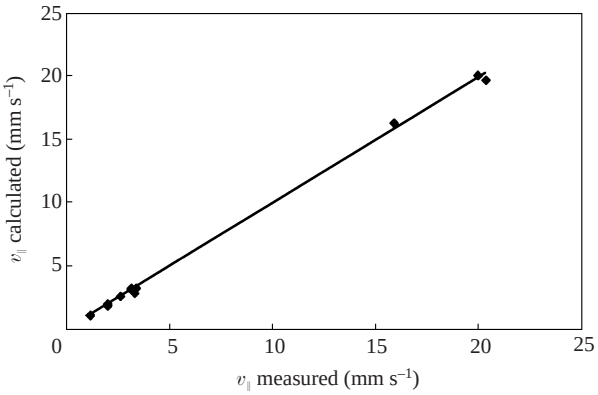

FIGURE 10. Experimental sedimentation velocities for models of arbitrary shape for vertical orientation ($v_\parallel$) plotted against velocities calculated using (2) together with the best-fit values of a and b. $y = 0.97x + 0.23$, $R^2 = 0.998$.

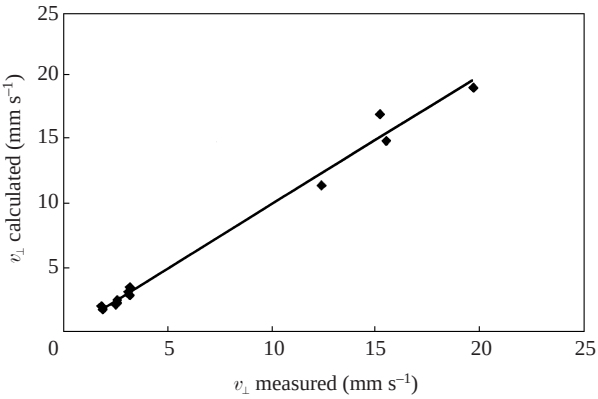

FIGURE 11. Experimental sedimentation velocities for models of arbitrary shape for instantaneous horizontal orientation ($v_\perp$) plotted against velocities calculated using (3) together with the best-fit values of a and b. $y = 1.007x - 0.15$, $R^2 = 0.99$.

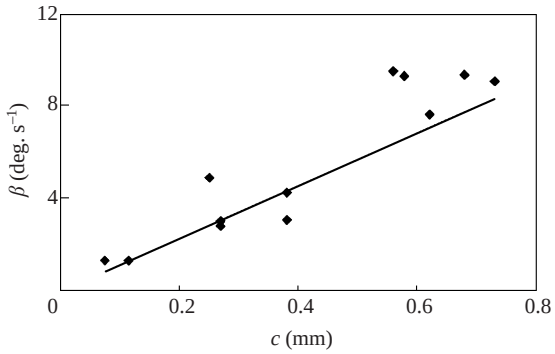

FIGURE 12. Values of β plotted against c for the models of arbitrary shape. Orientation rates have been scaled using (10) to a viscosity of 4.0 Pa s. The straight line shown on the graph is the theoretical prediction of (13), and the slope of the best-fit line to the experimental data is not significantly different ($P = 0.25$).

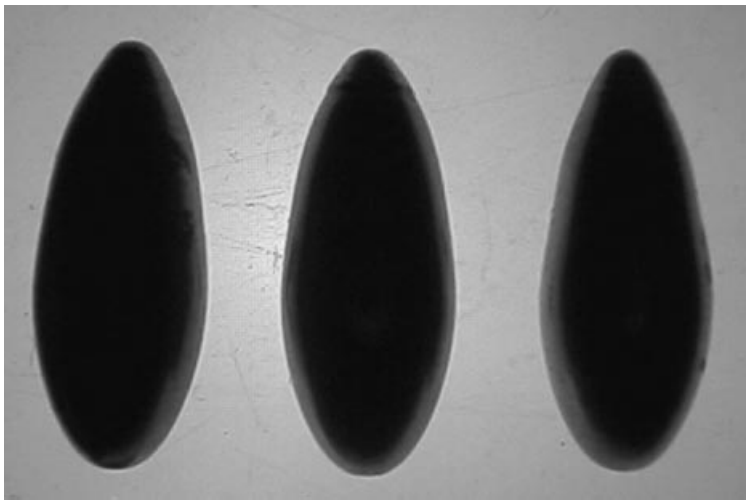

FIGURE 13. Photograph showing three models manufactured to the same nominal specifications. Their best-fit c/a values are very different, however, and the right-hand model (with $c/a = 0.088$) orientates almost 40% faster than the left-hand model (with $c/a = 0.064$) despite their similar-looking profiles.

example, is a ciliate which has a profile resembling that of *Paramecium caudatum* in one plane but is rather flattened in the perpendicular plane, and possesses less than a third of the volume of the latter (Nagel *et al.* 1997). Fortunately, organisms are not generally completely axially symmetrical, and tend to spin about their long axes as they swim. It should therefore be possible to obtain time-averaged profiles over one rotation to obtain average values for the asymmetry parameter c and hence estimate the magnitude of the overall orientation rate. It is not entirely clear how the effective profile of a cell that is covered with beating cilia, whose length is a significant fraction of the cell size, can be unambiguously identified. A further difficulty is that biological cells, even of the same species, show a wide range of sizes and shapes, so that a correspondingly wide range of sedimentation parameters is likely to exist in any given population. It may well be necessary to carry out careful observations on single cells in order to show clearly what mechanisms are involved in gravitaxis.

Comparison of microscope images of *Paramecium caudatum* with the outlines shown in figure 1 suggests that typical shape parameters might be $b/a = 0.3$ and $c/a = 0.05$. For a cell of length of $L = 220\,\mu\text{m}$, the corresponding values of a, b and c would be $110\,\mu\text{m}$, $33\,\mu\text{m}$ and $5.5\,\mu\text{m}$ respectively. Assuming a cell density of $1040\,\text{kg}\,\text{m}^{-3}$ and medium density and viscosity of $1000\,\text{kg}\,\text{m}^{-3}$ and $10^{-3}\,\text{Pa}\,\text{s}$ respectively (Nagel *et al.* 1997), then (3) gives $\beta = 0.12\ \text{rad}\,\text{s}^{-1}$, or about $7^\circ\,\text{s}^{-1}$. This value is in good agreement with the experimental range of results determined by Taneda & Miyata (1995). Individual cells possess a wide range of shapes, as mentioned earlier, and orientation rates will vary widely from cell to cell. Nevertheless, it suggests that shape orientation is playing the major role in gravitaxis, at least in this organism.

The model experiments demonstrate that the rate of orientation is very sensitive to small changes in shape (figure 13). This suggests that any procedure which indirectly affects the shapes of cells, such as the addition of metabolic agents, could also have a significant effect on gravitaxis via this simple physical mechanism. Such effects may not necessarily therefore be good evidence for the existence of specialized gravitational receptors in ciliates. Murakami (1998), for example, reports that a suspension of

Paramecium suddenly immersed in a high-density medium ($1080\,\mathrm{kg\,m^{-3}}$) first exhibits preferential downward swimming and reverts to normal upward swimming after 60 minutes. One possibility is that the shape and density of the cells may have changed due to the osmotic effects of the changed experimental medium. It also follows that sedimentation experiments on immobilized organisms are unlikely to yield meaningful results if the immobilizing treatment itself affects the shapes and internal density of the cells.

In flagellated organisms such as *Chlamydomonas* and *Euglena* the flagella that are used to propel the cells are themselves a potential cause of orientation in addition to any effects of body asymmetry. As the cell body sediments downwards it sinks beneath the protruding flagellum, thereby orientating the cell flagellum upwards, and, as figure 8 demonstrates, the maximum rate of orientation occurs when the length of the extended flagellum is about the same as that of the cell. The situation is complicated because a beating flagellum is constantly changing both its shape and its effective extension from the cell body. However, an approximate estimate can be obtained for the straight tail case.

Jones *et al.* (1994) give the following data for *Chlamydomonas*. The typical cell diameter (which is usually almost spherical) is $10\,\mu\mathrm{m}$, there are two flagella, each typically $10\,\mu\mathrm{m}$ long and of diameter $0.2\,\mu\mathrm{m}$, and the cell density is assumed to be $1050\,\mathrm{kg\,m^{-3}}$. The results of figure 8 cannot be used directly here because the model cell body is not spherical. However, experiments using models with spherical heads and tails of various lengths (Roberts 1975) showed that a creature with a spherical body of diameter $4\,\mu\mathrm{m}$ and density $1300\,\mathrm{kg\,m^{-3}}$, with a tail of length $4\,\mu\mathrm{m}$ and diameter $0.3\,\mu\mathrm{m}$, would orientate whilst sedimenting at the rate $\beta = 0.25\ \mathrm{rad\,s^{-1}}$. These results may be scaled using the scaling equation

$$\frac{\beta}{\beta_m} = \frac{\Delta\rho}{\Delta\rho_m}\frac{\eta_m}{\eta}\frac{L}{L_m}\frac{\ln(2T_m/b_m) + \frac{1}{2}}{\ln(2T/b) + \frac{1}{2}},$$

where T and b are the flagellum length and diameter, $\Delta\rho$ is the difference in density between cell and outside medium, η is the medium viscosity, and the subscript m refers to the model data. This equation is essentially (10) with a correction for the different flagellar diameters b based on Gray & Hancock's (1955) coefficients. Assuming that two widely separated flagella contribute twice the orientation that would be produced by one, the result for *Chlamydomonas* is that $\beta = 0.12\ \mathrm{rad\,s^{-1}}$.

The corresponding body shape orientation rate can be estimated using assumed shape data for the cell. *Chlamydomonas* is often depicted as being somewhat thinner at the front end (Jahn 1949) and comparison with the standard shapes in figure 1 suggests that $b/a = 0.4$ and $c/a = 0.08$ might be realistic values in this case. For $L = 10\,\mu\mathrm{m}$, $c = 0.4\,\mu\mathrm{m}$ and (13) yields a value for β of $0.01\ \mathrm{rad\,s^{-1}}$. This is significantly smaller than the estimated rate of flagellar orientation, as predicted earlier, and it may safely be concluded that body asymmetry is of little importance in small flagellates. Interestingly, orientation rates of about 0.3–0.4 $\mathrm{rad\,s^{-1}}$ have been measured in *Chlamydomonas* (Hill & Häder 1997) so flagellar orientation may be contributing about one third of the orientation, with a back-heavy mechanism contributing the remaining two-thirds.

Another much-studied flagellate, *Euglena gracilis*, has a long, narrow body, typically 35 to $55\,\mu\mathrm{m}$ in length, with a single anterior flagellum. The cell body often appears to be narrower at the rear, suggesting that shape orientation could cause the cell to swim downwards were it not for the opposing effects of the flagellum. At first sight

the scaling equation (14) implies that even in much larger cells possessing a single anterior flagellum the effects of body shape are likely to be swamped by the effects of the flagellum itself. However, *Euglena* tends to swim with its flagellum pointing at a slightly oblique angle to the cell's long axis (i.e. pointing slightly backwards), which will significantly reduce the degree of flagellar orientation. There may indeed in this case be a delicate balance between the effects of flagellar and shape orientation, with slight changes in flagellar beat pattern or cell shape causing marked changes in gravitaxis. This could be a simple physical mechanism whereby the reversals in gravitaxis observed by Lebert & Häder (1996, 1999) in *Euglena* could be accounted for.

It is concluded that shape-dependent orientation plays a major role in the gravitational responses of *Paramecium* and probably in other ciliates as well. The orientation rate is sensitively dependent on comparatively slight shape changes, and may explain why experiments to distinguish between alternative mechanisms have yielded equivocal results. In small flagellates the effects of flagellar orientation outweigh those of body shape, whilst in larger flagellates with trailing flagella the effects of body shape are probably equally important. It is difficult to see what evolutionary pressures could be responsible for the development of a specific gravity sensor in swimming micro-organisms. The whole cell may itself be acting as an elegant gravity sensor, with body shape and flagellar beat patterns playing a much more important role in the gravitational response of motile cells than has hitherto been supposed.

We are grateful to Mr R. Leary and his colleagues for constructing our computer-generated models, and to Dr W. Wang and our anonymous referees for their helpful comments.

REFERENCES

Bräucker, R., Murakami, A., Ikegaya, K., Yoshimura, K., Takahashi, K., Machemer-Ronisch, S. & Machemer, H. 1998 Relaxation and activation of graviresponses in *Paramecium caudatum*. *J. Expl Biol.* **201**, 2103–2113.

Childress, S., Levandowksy, M. & Spiegel, E. A. 1975 Pattern formation in a suspension of swimming micro-organisms: equations and stability theory. *J. Fluid Mech.* **63**, 591–613.

Dembowski, J. 1931 Die Vertikalbewegungen von *Paramecium caudatum*. *Archiv fur Protistenkunde* **74**, 153–187.

Fenchel, T. & Finlay, B. J. 1984 Geotaxis in the ciliated protozoan *Loxodes*. *J. Expl Biol.* **110**, 17–33.

Fukui, K. & Asai, H. 1980 The most probable mechanism of the negative geotaxis of *Paramecium caudatum*. *Proc. Japan Acad.* B *Phys. Biol. Sci.* **56**, 172–177.

Fukui, K. & Asai, A. 1985 Negative geotactic behaviour of *Paramecium caudatum* is completely described by the mechanism of buoyancy-oriented upward swimming. *Biophys. J.* **47**, 479–482.

Gray, J. & Hancock, G. J. 1955 The propulsion of sea-urchin spermatozoa. *J. Expl Biol.* **32**, 802–814.

Happel, J. & Brenner, H. 1973 *Low Reynolds Number Hydrodynamics*. Noordhoff.

Hemmersbach, R., Volkman, D. & Häder, D.–P. 1999 Graviorientation in protists and plants. *J. Plant Physiol.* **154**, 1–15.

Hill, N. A. & Häder, D.–P. 1997 A biased random walk model for the trajectories of swimming microorganisms. *J. Theor. Biol.* **186**, 503–526.

Jahn, T. L. 1949 *The Protozoa*. W. C. Brown, Iowa.

Jennings, H. S. 1906 *Behaviour of the Lower Organisms*. Indiana University Press.

Jones, M. S., Le Baron, L. & Pedley, T. J. 1994 Biflagellate gyrotaxis in a shear flow. *J. Fluid Mech.* **281**, 137–158.

Kessler, J. O. 1985 Hydrodynamic focusing of motile algal cells. *Nature* **313**, 218–220.

Kowalewski, R., Braucker, R. & Machemer, H. 1998 Responses of *tetrahymena pyriformis* to the natural gravity vector. *Microgravity Sci. Technol.* **XI/4**, 167-172.

Lebert, M. & Häder, D.-P. 1996 How *Euglena* tells up from down. *Nature* **379**, 590.

Lebert, M. & Häder, D.-P. 1999 Negative gravitactic behaviour of *Euglena gracilis* can not be described by the mechanism of buoyancy-orientated upward swimming. *Adv. Space Res.* **24**, 851–860.

Machemer, H. 1994 Gravity dependent modulation of swimming rate in ciliates. *Acta Protozoologica* **33**, 53–57.

Machemer, H. 1996 A theory of gravikinesis in *Paramecium*. *Adv. Space Res.* **17**, 6/7, 11–20.

Machemer, H., Machemer-Rohnisch, H., Bräucker, R. & Takahashi, K. 1991 Gravikinesis in *Paramecium*: theory and isolation of a physiological response to the natural gravity vector. *J. Comparative Physiol.* A **168**, 1–12.

Moore, A. 1903 Some facts concerning geotropic gatherings of *Paramecium*. *Am. J. Physiol.* **9**, 238–244.

Murakami, A. 1998 Short-term responses of gravitaxis to altered gravity in *Paramecium*. *Adv. Space Res.* **21**, 8/9, 1253–1261.

Nagel, U. & Machemer, H. 2000 Physical and physiological components of the graviresponses of wild-type and mutant *Paramecium tetraurelia*. *J. Expl Biol.* **203**, 1059–1070.

Nagel, U., Watzke, D., Neugebauer, D.-Ch., Machemer-Rohnisch, S., Braucker, R. & Machemer, H. 1997 Analysis of sedimentation of immobilized cells under normal and hypergravity. *Microgravity Sci. Technol.* **X/1**, 41–52.

Neugebauer, D. C., Machemer-Rohnisch, S., Nagel, U., Braucker, R. & Machemer, H. 1998 Evidence of central and peripheral gravireception in the ciliate *Loxodes striatus*. *J. Comput. Physiol.* **183**, 303–311.

Ooya, M., Mogami, Y., Izumi-Kurotani, A. & Baba, S.A. 1992 Gravity-induced changes in propulsion of *Paramecium caudatum*: A possible role of graviperception in protozoan behaviour. *J. Expl Biol.* **163**, 153–167.

Pedley, T. J., Hill, N. A. & Kessler, J. O. 1988 The growth of bioconvection patterns in a uniform suspension of gyrotactic micro-organisms. *J. Fluid Mech.* **195**, 223–237.

Pedley, T. J. & Kessler, J. O. 1987 The orientation of spheroidal micro-organisms swimming in a flow field. *Proc. R. Soc. Lond.* B **231**, 47–70.

Pedley, T. J. & Kessler, J. O. 1992 Hydrodynamic phenomena in suspensions of swimming micro-organisms *Annu. Rev. Fluid Mech.* **24**, 313–358.

Roberts, A. M. 1970 Geotaxis in motile micro-organisms. *J. Expl Biol.* **53**, 687–699.

Roberts, A. M. 1975 The biased random walk and the analysis of microorganism movement. In *Swimming and Flying in Nature* (ed. T. Y.-T. Wu, C. J. Brokaw & C. Brennen), vol. 1, pp. 377–394. Plenum Press.

Taneda, K. & Miyata, S. 1995 Analysis of motile tracks of *Paramecium* under gravity field. *Comput. Biochem. Physiol.* **111A**, 673–680.

Verworn, M. 1889 *Psychophysiologische Protistenstudien.* Fisher Verlag, Jena.

Wager, H. 1911 On the effect of gravity upon the movements and aggregation of *Euglena viridis* and other micro-organisms. *Phil. Trans. R. Soc. Lond.* B **201**, 333–390.